The EGFR-STAT3 Oncogenic Pathway Up-regulates the Eme1 Endonuclease to Reduce DNA Damage after Topoisomerase I Inhibition

Arnaud Vigneron, Erick Gamelin, and Olivier Coqueret

Cancer Center Paul Papin, Institut National de la Sante et de la Recherche Medicale U892, Université d'Angers, Angers, France

Abstract

The epidermal growth factor receptor (EGFR)-src-signal transducers and activators of transcription 3 (STAT3) oncogenic pathway plays a central role in tumorigenesis and is involved not only in cell transformation but also in tumor escape to genotoxic treatments. Despite its importance, the molecular mechanisms by which this signaling pathway induces resistance to DNA damage remain most of the time to be characterized. In this study, we show that the EGFR-src pathway is activated in response to topoisomerase I inhibition. After treatment, this signaling cascade induced the activation of STAT3 and the binding of the transcription factor to the promoter of the Eme1 gene. Eme1 is an endonuclease involved in the processing of DNA damage after topoisomerase I inhibition. These results suggest a model by which the STAT3-mediated activation of Eme1 prevents DNA damage and enhances cell survival in response to topoisomerase inhibition. This survival pathway was inhibited by a combined treatment with a src inhibitor, SKI, and with cetuximab, a monoclonal antibody directed against the EGFR that is widely used in the treatment of colorectal cancers. We therefore propose that the benefit of anti-EGFR therapy relies on an increase of DNA damage generated by topoisomerase I inhibition. [Cancer Res 2008;68(3):815–25]

Introduction

The epidermal growth factor receptor (EGFR) family consists of the EGFR, ErbB2/Neu, ErbB3, and ErbB4 proteins, which are activated after binding of several growth factors, such as EGF, transforming growth factor-α, or amphiregulin. Several studies have shown that activated forms of the receptor can induce cell transformation, and many epithelial cancers exhibit amplification, mutation, or autocrine activation of the EGFR, which in many cases, correlates with disease progression and poor prognosis. Targeted therapies interfering with EGFR signaling are now used as efficient strategies to increase the efficiency of conventional genotoxic treatments (1). Interfering with the EGFR oncogenic pathway is achieved through the use of either monoclonal antibodies or small molecule inhibiting its tyrosine kinase activity. Cetuximab (Erbitux; C225), a monoclonal antibody that binds to the EGFR, has been shown to inhibit the growth of several cancer cells *in vitro* and in nude mice (2). In addition, cetuximab potentiates the effect of genotoxic drugs such as the topoisomerase I inhibitor irinotecan (3–6). Most importantly, these preclinical results have been confirmed by clinical trials showing that the inhibition of the EGFR pathway through the use of cetuximab can reverse drug resistance, induce response, and prolong the survival of patients with irinotecan-refractory colorectal carcinoma (7, 8).

One essential question of cancer treatment is why tumors fail to respond to chemotherapy and which oncogenic signaling is predictive of tumor resistance. Unfortunately, the molecular mechanisms underlying the role of the EGFR pathway in refractory colorectal tumors remain to be characterized. The main pathways stimulated by the receptor are the mitogen-activated protein kinases (MAPK), the phosphatidylinositol 3-kinase–AKT, and signal transducer and activator of transcription proteins (STAT), such as STAT3 (9). In addition, the activation of STAT3 also relies on the recruitment of the src kinase to the EGFR (9–11). Upon nuclear translocation, the STAT3 transcription factor up-regulates several genes involved in cell cycle progression (12, 13), cell survival (14–18), and metastasis (19). Therefore, through the activation of src-STAT3, the EGFR signaling induces the expression of survival proteins such as Bcl-Xl or mcl1. These proteins are well-known to play an important role in drug resistance and tumor escape by inhibiting the cell death pathways associated with genotoxic treatments. Besides apoptosis, we have recently shown that the src-STAT3 oncogenes prevent senescence induction in response to genotoxic drugs through the up-regulation of Myc and the inactivation of the p53-p21 pathway (20). For these reasons, we have recently proposed that the STAT3 oncogenic signaling pathway plays an important role in drug resistance through the inactivation of tumor suppressor networks (21).

We now extend these observations and show in this study that the EGFR-src-STAT3 pathway is activated in response to topoisomerase I inhibition. After inhibition, DNA damage induced the activation of the src kinase, the activation of STAT3, and the binding of the transcription factor to the promoter of the Eme1 gene. Eme is an endonuclease identified as a member of the XPF family of endonucleases (22). This protein plays an important role in the processing of DNA repair after topoisomerase I inhibition, and its up-regulation confers resistance to several DNA-damaging agents. These results indicate that upon cell transformation, the EGFR-src-STAT3 oncogenic pathway induces the up-regulation of Eme1, thereby leading to an intrinsic drug resistance program. Consequently, the inactivation of the EGFR pathway by cetuximab prevents the expression of Eme1 and enhanced DNA damage and cell death in response to topoisomerase I inhibition. We propose that the benefit of cetuximab and anti-EGFR therapy relies on the

Note: Supplementary data for this article are available at Cancer Research Online (http://cancerres.aacrjournals.org/).

Current address for A. Vigneron: Beatson Institute for Cancer Research, Glasgow, United Kingdom.

Requests for reprints: Olivier Coqueret, Paul Papin Cancer Center, Institut National de la Sante et de la Recherche Medicale U892, Université d'Angers, 2 rue Moll, 49033 Angers, France. Phone: 33-2-41-35-27-00, ext. 2564; Fax: 33-2-41-48-31-90; E-mail: olivier.coqueret@univ-angers.fr.

doi:10.1158/0008-5472.CAN-07-5115

down-regulation of Eme1 expression and on the consequent increase of DNA damage generated by anticancer drugs, such as irinotecan, that induce an inhibition of topoisomerase I.

Altogether, these results reveal a complex network of interactions indicating that the EGFR-src-STAT3 oncogenic pathway induces the expression of the Eme1 endonuclease to induce cell transformation and drug resistance.

Materials and Methods

Materials. Antibodies were obtained from Santa Cruz Biotechnology. Anti-αtubulin (T9026) was obtained from Sigma, and Anti-Eme1 was obtained from Immuquest (IQ284). SKI was obtained from Calbiochem (#567805). The src siRNA was obtained from Santa Cruz (sc-29228), and SN38 comes from Pfitzer and Cetuximab from Merck. All cells were maintained in RPMI supplemented with 10% serum and were not used beyond 25 to 30 passages.

Chromatin immunoprecipitation assay. Attached cells were washed and cross-linked with 1% formaldehyde at room temperature for 10 min. Cells were washed sequentially twice with 1 mL ice-cold PBS, centrifuged, and then resuspended in 0.5 mL of lysis buffer [1% SDS, 10 mmol/L EDTA, 50 mmol/L Tris-HCl (pH 8.1), 1 mmol/L phenylmethylsulfonyl fluoride, 1 μg/mL leupeptin, and 1 μg/mL aprotinin] and sonicated thrice for 15 s each at the maximum setting. Supernatants were then recovered by centrifugation at 12,000 rpm for 10 min at 4°C, diluted twice in dilution buffer [1% Triton X-100, 2 mmol/L EDTA, 150 mmol/L NaCl, and 20 mmol/L Tris-HCl (pH 8.1)], and subjected to one round of immunoclearing for 2 h at 4°C with 2 μg sheared salmon sperm DNA, 2,5 μg preimmune serum, and 20 μL of protein A sepharose (of 50% slurry). Immunoprecipitation was performed overnight with specific antibodies, then 2 μg sheared salmon sperm DNA and 20 μL of protein A sepharose (of 50% slurry) were further added for 1 h at 4°C. Immunoprecipitates were washed sequentially for 10 min each in TSE I [0.1% SDS, 1% Triton X-100, 2 mmol/L EDTA, 20 mmol/L Tris-HCl (pH 8.1), and 150 mmol/L NaCl], TSE II [0.1% SDS, 1% Triton X-100, 2 mmol/L EDTA, 20 mmol/L Tris-HCl (pH 8.1), and 500 mmol/L NaCl], and buffer III [0.25 mol/LLiCl, 1% NP40, 1% deoxycholate, 1 mmol/L EDTA, and 10 mmol/L Tris-HCl (pH 8.1)]. Beads precipitates were then washed thrice with TE buffer and eluted twice with 1% SDS and 0.1 mol/L $NaHCO_3$. Eluates were pooled, heated at 65°C for 6 h to reverse the formaldehyde cross-linking, and DNA was precipitated using classic procedures. For PCR, 10 μL from a 100 μL DNA preparation were used for 25 to 30 cycles of amplifications. The amplified regions are presented on Fig. 5, and primers are available upon request.

Real-time PCR. For RNA quantification, PCR was performed with 5 μL of DNA and 5 pmol/L primers diluted in a final volume of 5 μL Reaction Mix lightcycler (Roche Diagnostics GmbH) and 4 mmol/L of $MgCl_2$. Accumulation of fluorescent products was monitored by real-time PCR using a lightcycler (Roche Diagnostics GmbH). The relative quantification of gene expression was performed using the comparative C_T method, with normalization of the target gene to the endogenous housekeeping gene glyceraldehyde-3-phosphate dehydrogenase (GAPDH).

Flow cytometry analysis. For DNA content analysis, 1×10^6 cells were washed twice with PBS and fixed in 70% ethanol. Cells were treated with 100 units/mL RNase A for 20 min at 37°C, resuspended in PBS containing 50 μg/mL propidium iodide, and immediately analyzed by flow cytometry (Becton Dickinson). For protein expression, 1×10^6 cells were washed twice with PBS, fixed in 70% ethanol, and further incubated for 45 min at 37°C in PBS containing 5% bovine serum albumin, 1 mg/mL RNase, and 2 μg/mL anti-H2AX (Upstate) or a control IgG. After three washes of PBS 0.1% Tween, cells were further incubated for 20 min with a FITC antibody at room temperature. After washes, samples were analyzed by flow cytometry. To quantify H2AX phosphorylation, result are presented as a ratio between the fluorescence with the H2Ax antibody and a control IgG: Fluo IgG H2AX/Fluo Control IgG.

Colony formation assay. For colony formation assay, 1.5 × 106 cells were plated per 10-cm plate and treated for the indicated times. Cells were then washed, trypsinized, and replated in drug-free medium in 6-well plates (diluted from 100,000 cells per well to 100 cells per well) and allowed to form colonies for 7 to 10 days. This corresponds to a hundred cells present in average in each colony. In parallel experiments, the percentage of senescent cells was determined by staining SA-β-gal activity using X-gal at pH 6.0. Cells were fixed in 0.25% glutaraldehyde in PBS for 15 min, washed thrice with PBS, and stained using fresh buffer [1 mg of 5-bromo-4-chloro-3-indolyl-β-D-galactoside/mL (stock 40 mg/mL DMSO), 5 mmol/L potassium ferrocyanide, 5 mmol/L potassium ferricyanide, 40 mmol/L citric acid sodium phosphate (pH 6.0), 150 mmol/L NaCl, 2 mmol/L $MgCl_2$, and PBS] at 37°C, for 16 to 20 h and in the absence of carbon dioxide. Positive cells were then counted by bright-field microscopy after scoring 100 to 1,000 cells for each sample.

Comet assay. A single-cell gel electrophoresis (Comet Assay) kit was used for evaluating DNA damage following the manufacturer's instructions (Trevigen, Inc.). After treatment of cells with DNA damage agents (i.e., SN38, cetuximab, or SKI), cells in 1× PBS ($Ca2^+$ and $Mg2^+$ free) at 1 × 105/mL were combined with molten LMAgarose (at 37°C) at a ratio of 1:10 (v/v) and immediately pipetted 75 μL onto CometSlideTM. After a gentle cell lysis, samples were treated with alkali to unwind and denature DNA. The samples were subjected to electrophoresis, stained with SYBR Green, and visualized by microscopy.

Results

The combined inhibition of src and EGFR sensitizes cell to topoisomerase I inhibition. We first tested the hypothesis that EGF-src signaling could act as a survival pathway in response to topoisomerase I inhibition. To this end, clonogenic assays were performed after exposure of colorectal cell lines to moderate doses of SN38, the active metabolite of irinotecan, which is widely used in the treatment of colorectal cancers. These experiments were performed in the presence or absence of the src inhibitor SKI and of cetuximab, a monoclonal antibody directed against the EGFR used in irinotecan-refractory colorectal carcinoma. Results presented in Fig. 1*A* showed that SN38 treatment resulted in 59% and 52% clonogenicity relative to untreated HCT116 and HT29 control cells, respectively. In the presence of cetuximab and SKI, a significant decrease of cell viability was observed compared with SN38 (Fig. 1*A*; compare *lanes 1* and *5*, *lanes 6* and *10*). Importantly, no effect of cetuximab or SKI was observed when added alone to the cell culture, and a nonrelated IgG did not affect cell proliferation. We also observed that the inhibition of the EGFR-src pathway decreased the concentration of SN38 required to reduce cell viability (Fig. 1*B*). The IC_{50} values were 1.6 ng/mL for SN38-treated HCT116 cells and 0.9 ng/mL in the presence of cetuximab-SKI, and 3.2 ng/mL for SN38-treated HT29 cells and 2.2 ng/mL in the absence of cetuximab-SKI.

To characterize the enhanced sensitivity to SN38, we then examined changes in senescence and apoptosis. The percentage of cells entering apoptosis was characterized by fluorescence-activated cell sorting (FACS) analysis (sub-G_1 fraction) and visual examination of condensed chromatin. The induction of the senescence program was detected by β-galactosidase staining and visual examination of the flattened phenotype. Micronucleation was characterized by micronuclei examination and detection of noncondensed chromatin in the main nuclei. In HCT116 cells, and as previously described (23), SN38 treatment results in the appearance of cells with multiple micronuclei, a hallmark of mitotic catastrophe. As a consequence, around 60% of the attached cells became senescent after 4 days of treatment (Fig. 1*C*, *left*). In the presence of cetuximab and SKI, a slight increase in SA-β-galactosidase–positive cells was noticed compared with the

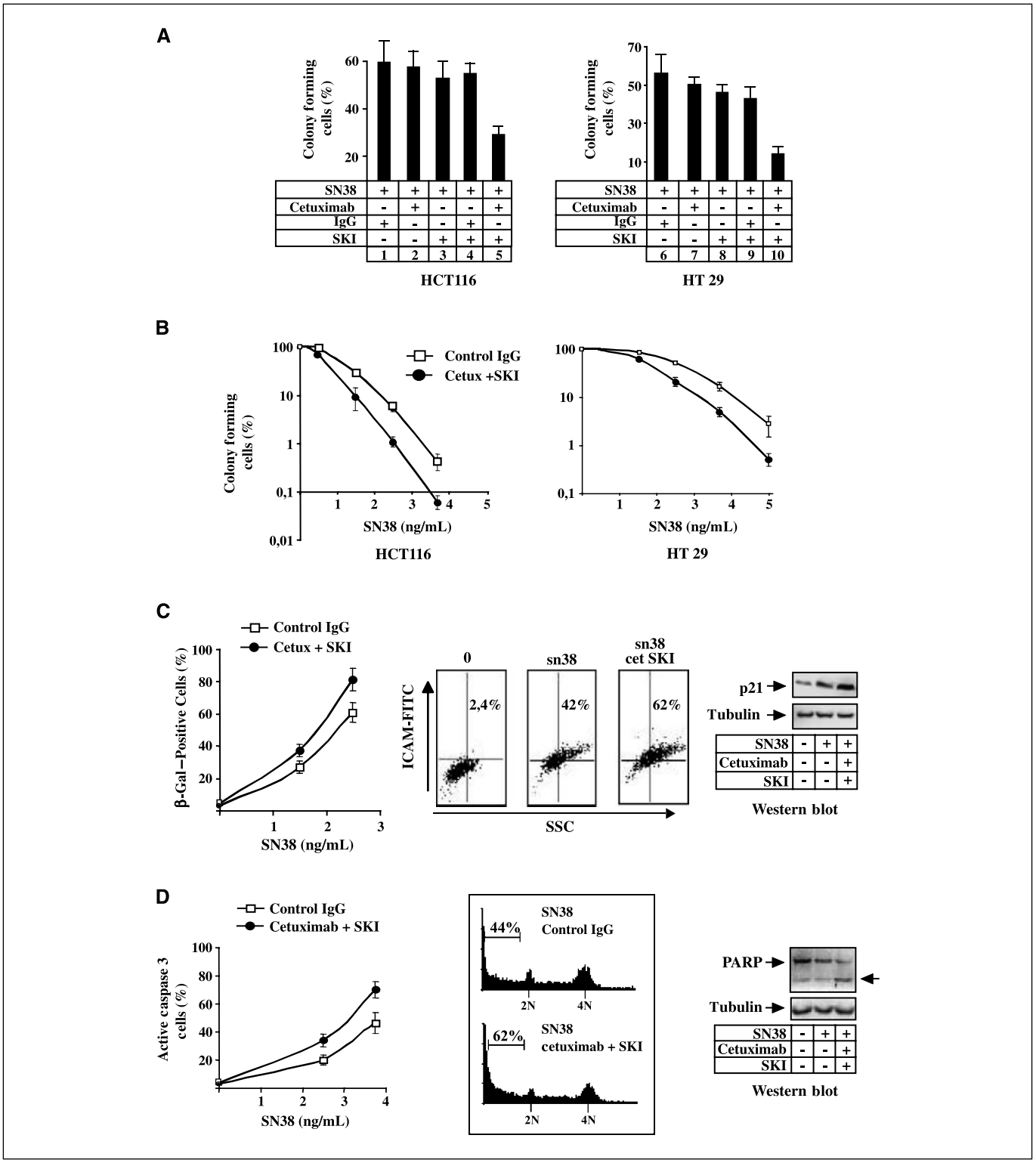

Figure 1. The combined inhibition of src and EGFR sensitizes cell to topoisomerase I inhibition. *A,* HCT116 or HT29 cells were treated with SN38 for 2 d in the presence or absence of cetuximab (*cetux*) and SKI as indicated, washed, replated, and further grown for 14 d [HCT116 (sn38: 2.5 nmol/L), HT29 (sn38: 3.7 nmol/L)]. Colony formation was then counted using an inverted microscope, and for each cell line, growth of nontreated cells was set up at 100%. Clonogenic survival was then plotted as a fraction relative to these untreated cells ($n = 3 \pm$ SD). *B,* colony formation was investigated as described in *A* in the presence of increasing concentrations of SN38 ($n = 3 \pm$ SD). *C,* growing HCT116 cells were treated with SN38 (2.5 nmol/L) for 48 h, in the presence or absence of cetuximab (2.5 μg/mL) and SKI (10 μmol/L) as indicated. The percentage of senescent cells was evaluated as the number of cells expressing SA-β-gal activity or by flow cytometry analysis using polyclonal antibodies directed against ICAM-1. In parallel, total cell extracts were prepared and analyzed by Western blot ($n = 3 \pm$ SD). *SSC*, side scatter. *D,* growing HT29 cells were treated with SN38 (3.7 nmol/L) for 48 h, in the presence or absence of cetuximab (2.5 μg/mL) and SKI (10 μmol/L) as indicated. After 36 h, the percentage of apoptotic cells was evaluated by flow cytometry using either polyclonal antibodies directed against the active form of caspase 3 or by FACS analysis of sub-G_1 cells. In parallel, total cell extracts were prepared and analyzed by Western blot ($n = 3 \pm$ SD). *PARP,* poly(ADP)ribose polymerase.

drug alone (Fig. 1*C, left*). To confirm this result, we evaluated the expression of the intercellular adhesion molecule-1 (ICAM-1), one of the markers overexpressed in senescent cells (24, 25). As expected, ICAM-1 was effectively induced by SN38 in HCT116 cells, and a significant up-regulation was noticed upon down-regulation of EGFR signaling (Fig. 1*C, middle*). After checkpoint arrest, senescence is also induced with the participation of the cell cycle inhibitor p21waf1. As expected, the SN38-mediated expression of p21waf1 was enhanced in the presence of cetuximab and SKI (Fig. 1*C, right*), indicating that EGFR-src inhibition up-regulates the induction of senescence.

We then determined if this effect was only related to the senescence pathway or also to other forms of cell death. To this end, we used HT29 cells because this cell line responds differently to genotoxic treatment and has a mutated form of p53, so that any effect would be independent of the tumor suppressor. In response to SN38, <10% of HT29 cells enter the senescence program or present micronuclei (data not shown; see also ref. 23). By contrast, apoptosis occurred in 35% to 40% of these cells in response to SN38, and this was enhanced upon inhibition of EGFR-src signaling (Fig. 1*D, left*). An increased in the percentage of sub-G_1 cells and of the cleavage of the poly(ADP)ribose polymerase protein was also observed in these conditions (Fig. 1*D, middle* and *right*). No effect was observed when cetuximab and SKI were added alone to the cell culture (data not shown).

Altogether, these results indicate that the inhibition of EGFR-src signaling potentiates the induction of senescence and apoptosis in response to topoisomerase I inhibition.

The inhibition of the EGFR-src signaling pathway induces DNA damage. SN38 induces topoisomerase I cleavage complexes that inhibit replication forks and induce DNA double strand breaks (26). Based on these observations, we made the hypothesis that

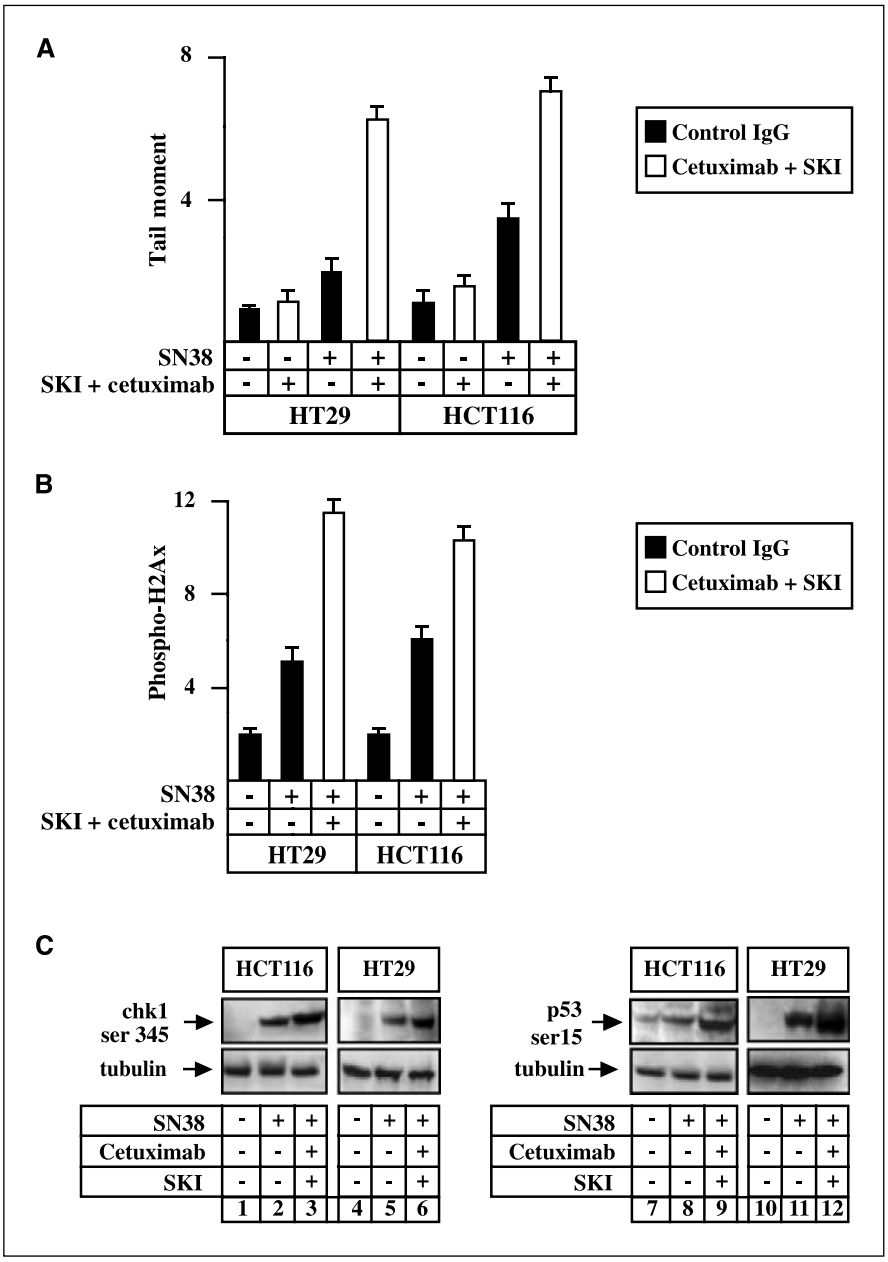

Figure 2. The combined inhibition of src and EGFR potentiates DNA damage induced by topoisomerase I (*topo1*) inhibition. *A,* HCT116 or HT29 growing cells were treated with SN38 for 24 h (HCT116, 2.5 nmol/L; HT29, 3.7 nmol/L), in the presence or absence of cetuximab (2.5 μg/mL) and SKI (10 μmol/L) as indicated. Cells were then washed and further treated for 12 h by cetuximab-SKI. The amount of DNA strand breaks was then determined using the alkaline comet assay and quantified using the Comet Assay IV software ($n = 3 \pm$ SD). *B,* HCT116 or HT29 growing cells were treated as described in *A*, and the generation of DNA double strand breaks was quantified by FACS analysis using polyclonal antibodies directed against the Ser^{139} phosphorylated form of γ-histone H2Ax ($n = 3 \pm$ SD). *Phospho-H2Ax*, histone H2Ax phosphorylation. *C,* cells were treated as described in *A*, and total cell extracts were prepared and analyzed by Western blot ($n = 3$).

Table 1. Regulation of DNA repair genes after inhibition of the EGFR-src pathway

	HCT116		HT29			HCT116		HT29	
	src+	src−	src+	src−		src+	src−	src+	src−
NER					Recombination				
ERCC1	2.15	0.89	1.82	1.12	Holiday junction resolution				
XPF	0.87	1.04	1.12	1.23	Rad51	2.23	1.87	2.98	3.12
XPG/ERCC5	2.89	3.45	4.14	3.85	XRCC2	1.84	1.87	1.68	1.79
XPC	1.54	1.65	1.79	1.67	XRCC3	3.45	4.23	4.23	4.75
XPA	1.97	2.03	0.84	1.02	BLM	2.21	2.03	2.45	2.2
					WRN	3.21	3.12	2.89	3.45
NHEJ					BRCA2	3.21	3.12	2.89	3.45
XRCC4	0.52	0.46	0.77	0.64	TOP3	1.44	1.56	3.12	3.06
exo1	1.02	1.23	0.94	0.92	Mus81	0.98	1.15	0.84	0.94
					Eme1	4.52	1.7	4.89	1.62
DNA damage									
Sensor/transducer					TOPO I processing complex				
NBS1	0.94	0.92	0.85	1.23	Fen1	2.1	1.31	1.34	0.48
Rad50	1.26	1.12	0.78	0.84	TOPO I	1.12	0.95	1.23	1.17
MRE11	1.51	1.31	1.13	1.23	PNPK	1.23	0.95	0.84	0.78
rpa2	2.9	2.4	3.8	4.1	XRCC1	0.84	0.74	1.54	0.91
BRCA1	2.1	2.3	2.82	2.9	TDP1	1.42	1.12	1.48	0.98
Rad17	0.8	0.84	1.77	1.99					

NOTE: HCT116- or HT29-growing cells were treated with SN38 for 24 h (HCT116, 2.5 nmol/L; HT29, 3.7 nmol/L), in the presence or absence of cetuximab (2.5 μg/mL) and SKI606 (10 μmol/L; indicated src+ or src− for simplicity on the table). Cells were then washed and further treated for 12 h by cetuximab-SKI606. The expression of the indicated mRNAs was then evaluated by quantitative RT-PCR experiments (n = 5).

EGFR-src inhibition might potentiate the effect of SN38 on DNA damage. To verify this, genotoxicity analysis were performed using either the alkaline comet assay (Fig. 2*A*) or Ser^{139} phosphorylation of histone H2Ax as a marker of DNA double strand breaks (Fig. 2*B*). As expected, SN38 treatment led to a significant increase of the tail moment in HT29 and HCT116 cells. Accordingly, FACS analysis also showed an increase in γ-H2Ax phosphorylation, confirming that DNA double strand breaks occurred in SN38-treated cells (Fig. 2*B*). Importantly, when cetuximab and SKI were added to the cell cultures, we observed that the inhibition of the EGFR-src signaling pathway further enhanced DNA damage. As shown Fig. 2*A*, an increased tail moment was observed in the presence of cetuximab and SKI both in HT29 cells (tail moment, 6.3 ± 1.4 for treated cells; compared with SN38 alone tail moment, 2.2 ± 0.6) and HCT116 cells (tail moment, 6.9 ± 1.6 for treated cells; compared with SN38 tail moment, 3.7 ± 0.4). Accordingly, FACS analysis indicated that the Ser^{139} phosphorylation of H2Ax was also enhanced after EGFR-src inhibition (Fig. 2*B*). To confirm these results, we then analyzed the activation of DNA damage checkpoints in drug-treated cells (Fig. 2*C*). After genotoxic treatment of HCT116 and HT29 cells, we observed that the chk1 kinase was phosphorylated on its Ser^{345} residue. In addition, SN38 also induced the phosphorylation of p53 on Ser^{15} in both cell lines. Confirming the above results, the activation of chk1 and p53 was enhanced when the EGFR-src pathway was inhibited (Fig. 2*C, lanes 3, 6, 9*, and *12*). Importantly, kinetic experiments indicated that EGFR inhibition had no significant effect on DNA damage after 24 h of treatment (data not shown). Looking at tail moments or γ-H2Ax phosphorylation, DNA damage induction became detectable only when cells were allowed to proliferate for a further 12 h in the presence of cetuximab and SKI (Fig. 2). In addition, we have also observed that the length of S phase is not modified after cetuximab-SKI treatment. This might indicate that EGFR inhibition affects late S phase or G_2 events that occur after topoisomerase I inhibition, such as the processing of collapsed replication forks and/or the processing of the D loop generated during the recombination process (27).

Taken together, these results suggest that the inhibition of the EGFR-src signaling pathway induced cell death through enhanced DNA damage.

The EGFR-src signaling pathway regulates the expression of the Eme1 endonuclease. Having shown that the inhibition of the EGFR-src pathway increased DNA damage, we then determined if this effect was related to a reduced expression of genes involved in the repair/signaling or processing of DNA breaks. Using quantitative reverse transcription-PCR (RT-PCR) experiments, we observed as expected that several genes involved in DNA repair pathways were up-regulated by >2-fold in response to topoisomerase I inhibition (Table 1). Although EGFR-src inhibition did not affect the majority of these regulators, we noticed that the expression of the Eme1 gene was significantly down-regulated upon inhibition of EGFR signaling (Table 1). Eme1 is an endonuclease that is implicated in the efficient rescue of broken replication forks in yeast. Importantly, Eme1 inactivation has been correlated with elevated levels of DNA damage, chromosomal aberrations, and drug sensitivity (22, 28). In HCT116 and HT29 cells, Western blot and quantitative PCR experiments showed that Eme1 expression was significantly induced in response to SN38 (Fig. 3*A* and *B*). Importantly, this up-regulation was almost completely inhibited

upon EGFR-src down-regulation (Fig. 3*A, lanes 3* and *6*). As a control, no effect was noticed on the expression of other DNA repair genes, such as xrrc1 or fen1, and a nonrelated IgG had no effect on Eme1 expression (data not shown).

Altogether, these results indicate that the Eme1 endonuclease is up-regulated by the EGFR pathway upon topoisomerase I inhibition.

DNA damage induced the phosphorylation of the EGF receptor. During the course of these experiments, we observed that the EGFR pathway was surprisingly activated upon topoisomerase I inhibition. As depicted in Fig. 4*A*, an increased phosphorylation of the intracellular domain of the EGFR was observed after drug exposure of HCT116 cells (Fig. 4*A, lanes 1–2*). In addition, topoisomerase I inhibition also induced the phosphorylation of the src kinase on its Tyr^{419}-activating residue (Fig. 4*A, lanes 3–4*). Importantly, this EGFR phosphorylation was inhibited by pretreatment exposure with SKI and with cetuximab in HCT116 and HT29 cells (Fig. 4*B*; compare *lanes 2* and *5, lanes 7* and *10*). Under these conditions, a significant inhibition of src phosphorylation was also observed (Fig. 4*C, lanes 3* and *6*). Again, when these two inhibitors were used alone, no significant effect was observed on the SN38-mediated activation of the EGFR. As a control, herceptin, a monoclonal antibody directed against the HerII receptor, did not affect the phosphorylation of the receptor (Fig. 4*B, lanes 11–16*). Because the EGFR-scr pathway activates STAT3, we then asked if the transcription factor was activated under the same conditions. Western blot experiments showed that SN38 induced the phosphorylation of STAT3 on its Ser^{727} residue in HCT116 and HT29 cells (Fig. 4*D, lanes 3* and *6*). As expected, the phosphorylation of STAT3 was inhibited in the presence of SKI and cetuximab, whereas the phosphorylation of the Akt kinase was not affected.

Altogether, these results indicate that the EGFR-src-STAT3 signaling pathway is activated upon topoisomerase I inhibition.

The STAT3 transcription factor is activated by SN38 to bind to the Eme1 promoter. In light of these results, we speculated that the EGFR-src cascade regulates the expression of Eme1 through STAT3 activation. Transcription factor recognition site analysis of the Eme1 promoter (MatInspector; Genomatix) revealed the presence of a potential STAT3 binding site in the proximal promoter of the gene (Fig. 5*A, left*). To determine if STAT3 is associated with this promoter in response to SN38, chromatin immunoprecipitation (ChIP) experiments were then performed using STAT3 antibodies. Ets1 antibodies were used as controls because a potential ets1 binding site was also found in this region. ChIP experiments indicated that STAT3 was significantly recruited to the proximal Eme1 promoter upon SN38 stimulation (Fig. 5*A, right*). Importantly, the association of the transcription factor with DNA was significantly prevented after EGFR-src inhibition. As a control, PCR analysis did not detect any occupancy of the exon 2 of

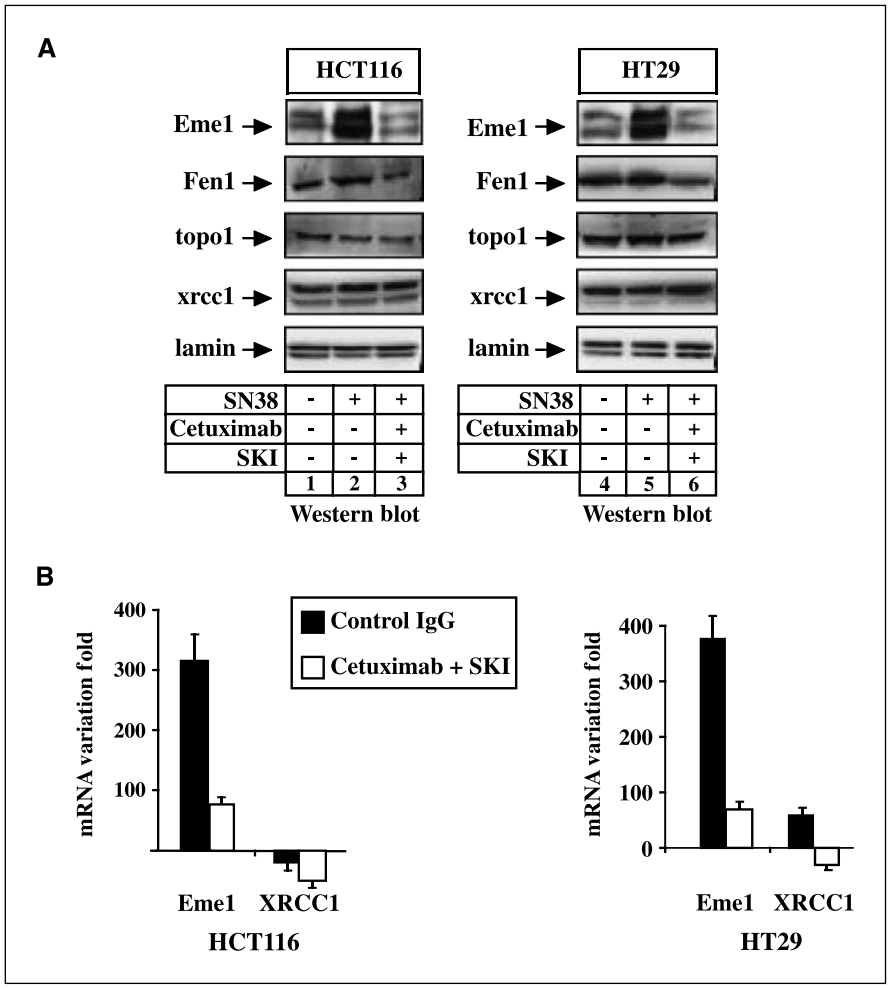

Figure 3. The inhibition of the EGFR-src pathway prevents the expression of the Eme1 endonuclease in response to topoisomerase I inhibition. *A,* HCT116- or HT29-growing cells were treated with SN38 for 36 h (HCT116, 2.5 nmol/L; HT29, 3.7 nmol/L), in the presence or absence of cetuximab (2.5 μg/mL) and SKI (10 μmol/L) as indicated. Total cell extracts were prepared and analyzed by Western blot ($n = 3$). *B,* cells (HCT116, *left*; HT29, *right*) were treated as described above for 24 h, and the expression of the indicated mRNA was analyzed by quantitative RT-PCR experiments ($n = 3 \pm$ SD).

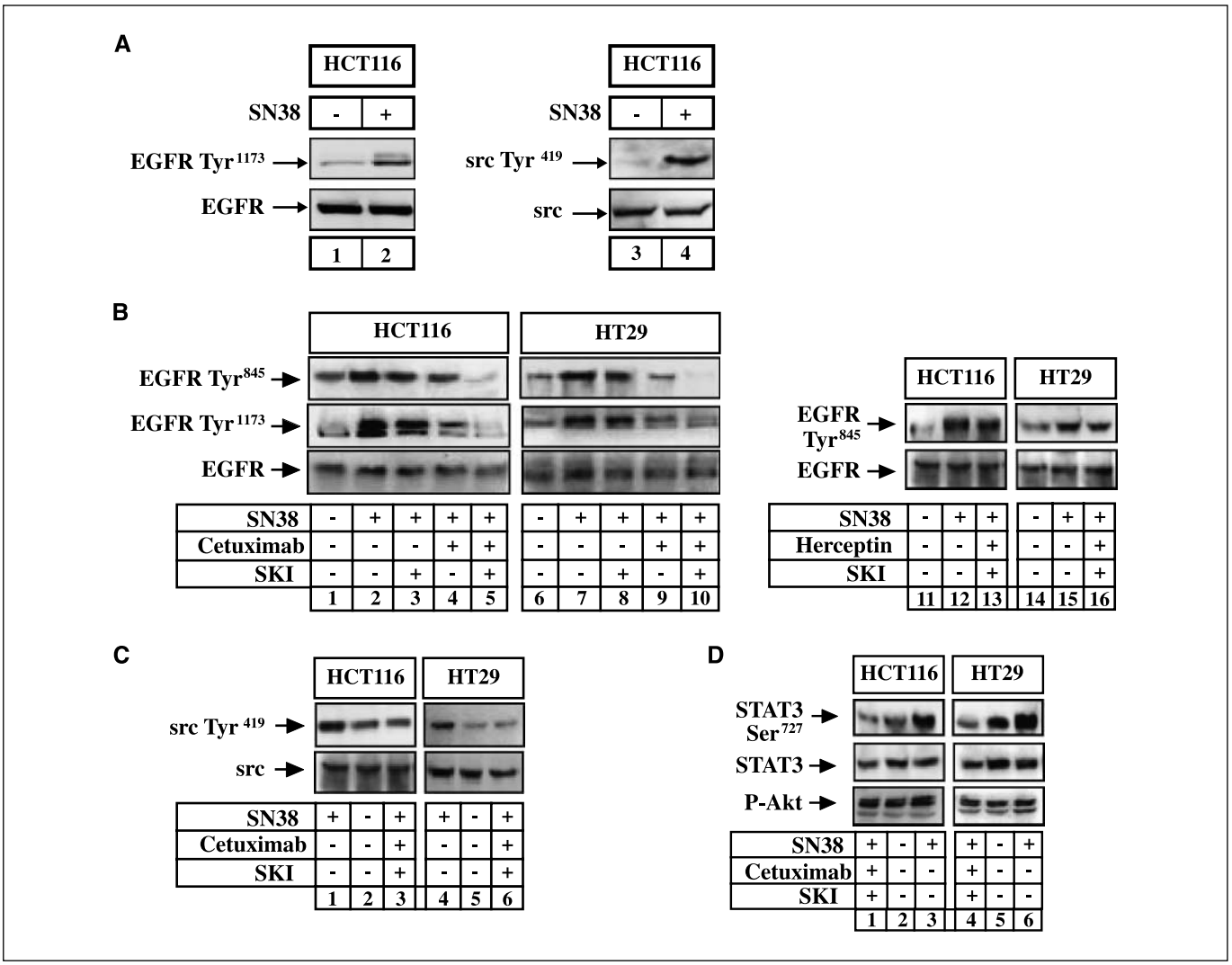

Figure 4. Topoisomerase I inhibition induced the phosphorylation of the EGFR-src pathway. *A* to *C,* growing cells were treated with SN38 for 24 h (HCT116, 2.5 nmol/L; HT29, 3.7 nmol/L), in the presence or absence of cetuximab (2.5 μg/mL) or SKI (10 μmol/L) as indicated. Herceptin (anti-Erb2, 2.5 μg/mL) was used as a control. Total cell extracts were prepared and analyzed by Western blot with antibodies directed against the phosphorylated forms of the EGFR or src as indicated (n = 3). *D,* HCT116 or HT29 growing cells were treated with SN38 for 36 h (HCT116, 2.5 nmol/L; HT29, 3.7 nmol/L), in the presence or absence of cetuximab (2.5 μg/mL) and SKI (10 μmol/L) as indicated. Total cell extracts (including the chromatin fraction) were then prepared, and Western blot experiments were performed with the indicated antibodies (n = 3).

the GAPDH gene by STAT3 (Fig. 5*B, left*). In addition, we have also been unable to detect any binding of the ets1 transcription factor to the proximal promoter of the Eme1 gene, further confirming the specificity of STAT3 recruitment (Fig. 5*B, right*).

We have recently shown that STAT3 binds to the promoter of the Myc gene upon IL-6 stimulation, a condition that is well-known to induce the transition from quiescence to the G_1 phase of the cell cycle. In the experimental conditions used in this study, FACS analysis indicated that SN38 induced an accumulation of cells in the G_2 phase of the cell cycle (Fig. 5*C, left*). To confirm the specificity of STAT3 activity, cells were treated with IL-6 to determine if this cytokine could also induce the activation of the Eme1 gene. As expected, IL-6 induced the binding of STAT3 to the Myc promoter (Fig. 5*C, middle*) and the consequent up-regulation of the Myc mRNA (data not shown; see ref. 12). By contrast, IL-6 did not induce the association of STAT3 with the Eme1 promoter (Fig. 5*C, middle*), and consequently, this cytokine had no effect on Eme1 mRNA levels (data not shown). Conversely, although STAT3 can be found associated with the Eme1 promoter upon SN38 stimulation, no binding could be detected on the Myc promoter under these conditions (Fig. 5*C, right*).

Altogether, these results indicate that STAT3 is specifically activated by topoisomerase I inhibition to induce the expression of the Eme1 endonuclease.

The EGFR-src-STAT3 pathway prevents DNA damage through Eme1 up-regulation. Altogether, these results indicate that the EGFR-src pathway activates STAT3 upon topoisomerase I inhibition, and that this leads to Eme1 up-regulation and resistance to DNA damage. To verify this hypothesis, cells were transfected with a siRNA directed against src, and the expression of Eme1 as well as histone H2Ax phosphorylation were then investigated in the presence or absence of SN38 and cetuximab. After siRNA transfection, we observed as expected that src expression was down-regulated, and that the phosphorylation of STAT3 on its

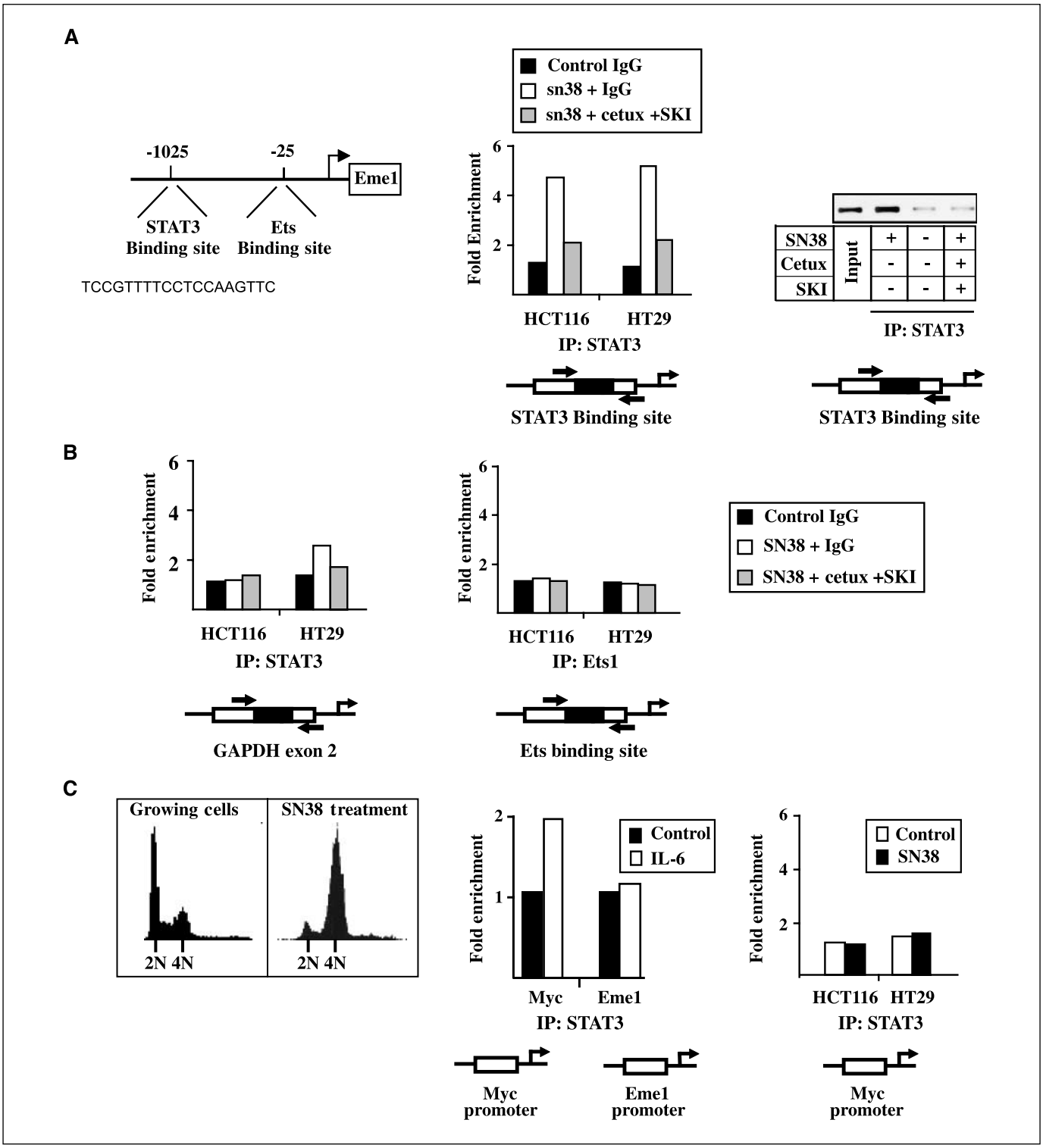

Figure 5. The STAT3 transcription factor is activated in response to topoisomerase I inhibition to induce the expression of the Eme1 gene. *A,* representation of the STAT3 and ets1 binding site on the Eme1 promoter (*left*). HCT116 or HT29 growing cells were treated as described above, and soluble chromatin was prepared from the indicated cells and immunoprecipitated with antibodies directed against the nonphosphorylated form of STAT3. DNA was amplified using one pair of primers that covers the STAT3 binding site of the Eme1 promoter. ChIP assays were analyzed by RT-PCR, and the percentage of immunoprecipitated DNA was calculated by comparison to input signals ($n = 3$; middle part of the figure). A representative agarose gel of the STAT3 ChIP on the Eme1 promoter is shown on the right part of the figure. *B,* ChIP experiments were performed as decribed above and analyzed using a pair of primers that covers the GAPDH gene as a control. In parallel, the association of the ets1 transcription factor with the Eme1 promoter was analyzed by ChIP in growing cells or in cells that were treated as decribed above ($n = 3$). *C,* HT29 cells were treated or not with SN38 for 36 h. FACS analysis was then performed on the indicated attached cells after propidium iodide staining. In parallel, cells were serum starved for 2 d and stimulated with IL-6 (10 ng/mL) for 30 min as indicated. ChIP experiments were then performed to detect the association of STAT3 with the Eme1 gene or with the Myc proxymal promoter (region −333/−44; relative to the P2 promoter). In addition, growing cells were treated with SN38 for 36 h, and the association of STAT3 with the Myc promoter was analyzed by ChIP experiments (*right*; $n = 3$).

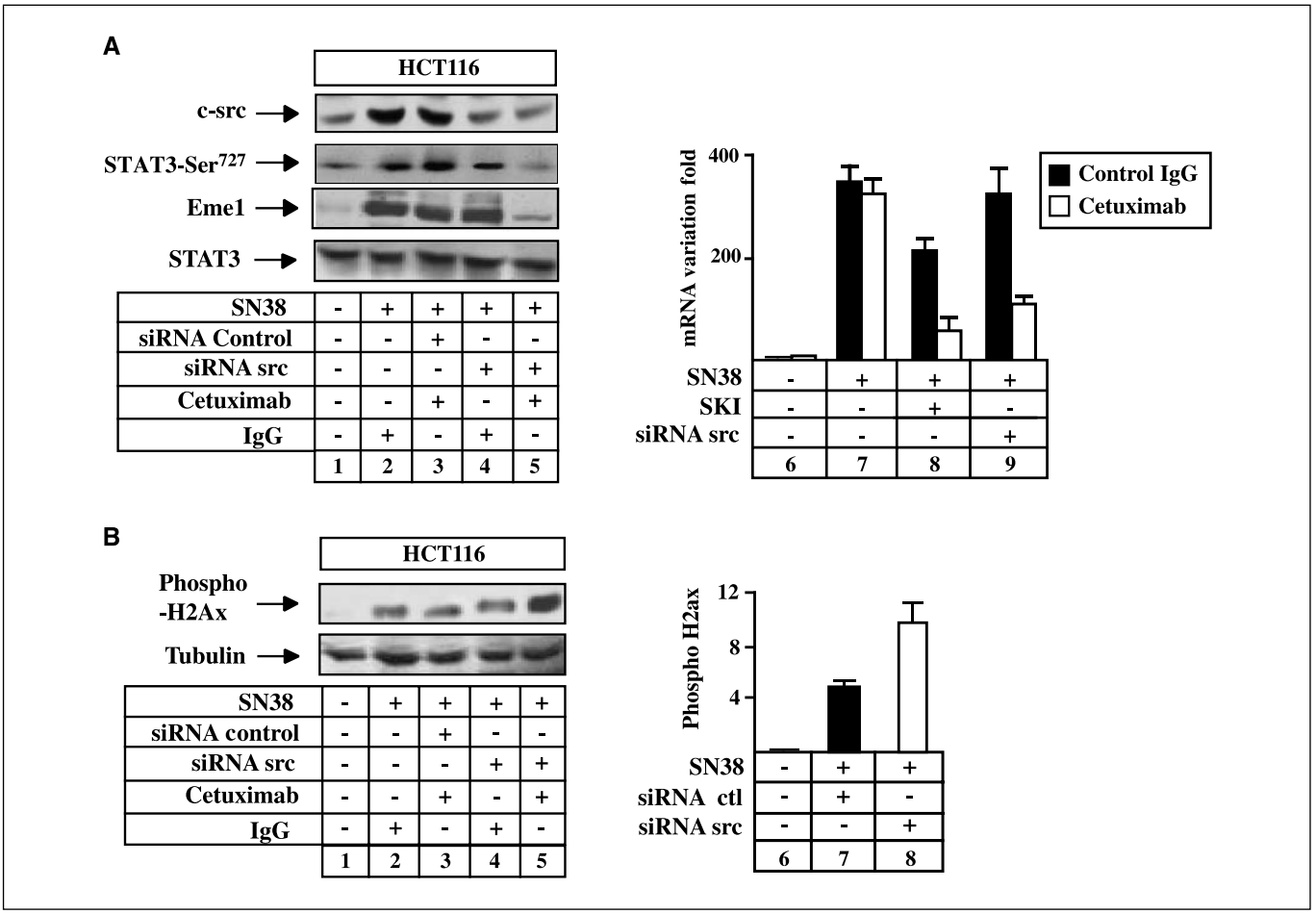

Figure 6. The EGFR-src-STAT3 pathway prevents DNA damage through Eme1 up-regulation. *A,* HCT116 cells were either transfected with src-specific siRNA oligonucleotides or control oligonucleotides, and expression was monitored after treatment with SN38 (2.5 nmol/L), in the presence or absence of cetuximab. Cells were treated for 24 h, washed, and then allowed to grow for a further 12 h. Total cell extracts were probed for the expression of src, STAT3, and Eme1 using polyclonal antibodies. In parallel, the expression of the Eme1 mRNA was analyzed by quantitative RT-PCR experiments (*right*; $n = 3 \pm$ SD). *B,* cells were treated as described in *A*, and DNA damage was monitored by Western blot analysis using histone H2Ax phosphorylation (*Phospho-H2Ax*) as a marker of double strand breaks (*left*). In parallel, DNA damage was quantified by FACS analysis (*right*; $n = 3 \pm$ SD).

Ser^{727} residue was inhibited upon genotoxic treatment (Fig. 6*A, lanes 1–5*). Importantly, we also observed that the combined inhibition of EGFR and src prevented the expression of Eme1 in response to SN38 (Fig. 6*A*; compare *lane 5* and *2*). Using quantitative PCR experiments, we also noticed that the siRNA-mediated inhibition of src prevented the expression of the Eme1 mRNA (Fig. 6*A, lanes 6–9*). As a control, no significant modification of the expression level of other DNA repair genes such as Tdp1 and Fen1 was observed (data not shown). Interestingly, src down-regulation also led to an increased DNA damage. Western blot experiments showed that the siRNA-mediated down-regulation of the kinase induced a very significant increase of histone H2Ax phosphorylation compared with the effect of SN38 alone (Fig. 6*B*; compare *lane 2* and *5*). The same effect was also observed when histone H2Ax phosphorylation was quantified using FACS analysis (Fig. 6*B, lanes 6–8*), probably illustrating the consequence of DNA double strand breaks induced by Eme1 inhibition. Kinetic experiments indicated under these conditions that EGFR inhibition did not induce DNA damage during the first 24 h. DNA damage became detectable only when the cells were washed and allowed to grow for a further 12 h. This again suggest that essentially late S phase or G_2 events were affected by the inhibition of EGFR signaling.

Therefore, we concluded from these results that the EGFR-src pathway prevents DNA damage in response to topoisomerase I inhibition through up-regulation of the Eme1 gene.

Discussion

It has been proposed that certain oncogenes may provide cancer cells with an inherent resistance mechanism to anticancer drugs (29, 30). Illustrating this hypothesis, we have recently shown that the src-STAT3 oncogenes inactivate senescence through Myc up-regulation and inactivation of the p53-p21 pathway (20). In addition to tumor suppressor inactivation, the ability of cancer cells to survive to genotoxic treatments also relies on the efficacy of their DNA repair pathways (31). In this study, we extend the functions of the EGFR-src-STAT3 oncogenes in drug resistance and show that this pathway up-regulates the expression of the Eme1 endonuclease. Illustrating the potential of targeted therapies, the combined inhibition of the src and EGFR kinases by SKI and cetuximab potentiates the effect of the topoisomerase I inhibitor

SN38 on cell death. This effect was shown to result from Eme1 down-regulation and enhanced DNA damage.

The Mus81-Eme1 complex was initially characterized in yeast as a member of the XPF family of endonuclease complexes involved in the repair of replication and meiotic defects. By analogy to XPF-ERCC1, Eme1 needs to associate with its Mus81 partner to form an active heterodimer complex that plays an important role in the repair and/or processing of postreplication damage. Further experiments need to be performed to determine if the EGFR signaling is involved in parallel in the regulation of the Mus81 gene. After genotoxic treatment and replication blockade, Mus81-Eme1 removes the collapsed replication forks and activates the homologous recombination process (27). As a consequence, the overexpression of the Mus81-Eme1 complex confers resistance to agents that block replication forks such as hydroxyurea and topoisomerase I inhibitors. In addition, its inactivation has been shown to induce genomic instability and enhance the sensitivity to DNA cross-linking agents (28, 32). We therefore propose that a high expression of Eme1 due to STAT3 activation represents an intrinsic drug resistance program that allows EGFR-scr–expressing tumors to respond to topoisomerase I inhibitors. Importantly, the combined inhibition of src and EGFR with SKI-cetuximab inactivates STAT3 and down-regulates the expression of Eme1. Although this remains to be shown, this treatment should prevent the processing of topoisomerase I cleavage complexes during G_2 arrest. Because colorectal cancer cells are able to adapt to G_2 DNA damage checkpoints (33, 34), we speculate that drug adaptation in response to SKI-cetuximab allows the progression of SN38-treated cells toward mitosis. The detection of broken forks and damaged chromosomes by the spindle checkpoint would then induce cell death through the up-regulation of control proteins such as BubR1, Mad1, or Mad2 (35). By contrast, in the absence of cetuximab-SKI, a normal up-regulation of Eme1 in SN38-treated cells would allow a more efficient processing of cleavage complexes. As a consequence, a higher percentage of cells would resume proliferation during the G_2 phase of the cell cycle, allowing tumor escape to cell death and mitotic checkpoint.

Further experiments need also to be performed to determine how DNA damage and topoisomerase I inhibition induce the activation of the EGFR-src pathway. Previous studies have already suggested that the EGFR is activated by osmotic and oxidative stresses through metalloprotease cleavage of EGF-like ligand precursors (36). This EGFR signal resulted from stress-induced activation of the ADAM family of metalloproteases and is mediated by the MAPK p38. Interestingly, DNA damage induced by cisplatin also leads to the phosphorylation of the EGFR and this effect is also mediated by p38 MAPK (37). Altogether, these observations lead to the interesting hypothesis that the up-regulation of Eme1 by STAT3 could result from the activation of the p38-ADAM pathway by topoisomerase I inhibition. In addition, it remains also to be determined if the EGFR pathway could also up-regulate the expression of Eme1 through mRNA or protein stabilization.

Altogether, these results uncover new functions for the STAT3 oncogenic pathway in the regulation of DNA repair. Although this remains to be firmly established, we therefore propose that the EGFR-src-STAT3 oncogenic pathway up-regulates Eme1 expression to allow a more efficient processing of cleavage complexes and to induce drug resistance (Supplementary Fig. S1). Because an important correlation exists between EGFR, src, STAT3, and colorectal cancers, our results suggest that tumors expressing the EGFR-src-STAT3 pathway together with a high expression of Eme1 might be resistant to DNA–topoisomerase I inhibitors such as irinotecan. For these reasons, the detection of these proteins should help to determine the drug resistance profile of individual tumors to define in advance the subsets of tumors that will fail to respond to chemotherapy. Provided that this combination does not lead to serious side effects, we propose that cetuximab and src inhibitors should be used as targeted therapies with topoisomerase I inhibitors to sensitize drug-resistant colorectal tumors to cell death.

Acknowledgments

Received 8/31/2007; revised 11/20/2007; accepted 11/28/2007.

Grant support: A fellowship (A. Vigneron), a grant from the Ligue contre le Cancer (Equipe labélisée 2007–2010; O. Coqueret), and a grant from Assocation pour la Recherche sur le Cancer (ARC 2005–2007, #3133).

The costs of publication of this article were defrayed in part by the payment of page charges. This article must therefore be hereby marked *advertisement* in accordance with 18 U.S.C. Section 1734 solely to indicate this fact.

We thank Philippe Juin and Neil Perkins for a critical reading of the manuscript.

References

1. Hynes NE, Lane HA. ERBB receptors and cancer: the complexity of targeted inhibitors. Nat Rev Cancer 2005; 5:341–4.
2. Galizia G, Lieto E, De Vita F, et al. Cetuximab, a chimeric human mouse anti-epidermal growth factor receptor monoclonal antibody, in the treatment of human colorectal cancer. Oncogene 2007;26:3654–60.
3. Kim S, Prichard CN, Younes MN, et al. Cetuximab and irinotecan interact synergistically to inhibit the growth of orthotopic anaplastic thyroid carcinoma xenografts in nude mice. Clin Cancer Res 2006;12:600–7.
4. Ciardiello F, Bianco R, Damiano V, et al. Antitumor activity of sequential treatment with topotecan and anti-epidermal growth factor receptor monoclonal antibody C225. Clin Cancer Res 1999;5:909–16.
5. Huang SM, Bock JM, Harari PM. Epidermal growth factor receptor blockade with C225 modulates proliferation, apoptosis, and radiosensitivity in squamous cell carcinomas of the head and neck. Cancer Res 1999;59: 1935–40.
6. Prewett MC, Hooper AT, Bassi R, et al. Enhanced antitumor activity of anti-epidermal growth factor receptor monoclonal antibody IMC-C225 in combination with irinotecan (CPT-11) against human colorectal tumor xenografts. Clin Cancer Res 2002;8:994–1003.
7. Cunningham D, Humblet Y, Siena S, et al. Cetuximab monotherapy and cetuximab plus irinotecan in irinotecan-refractory metastatic colorectal cancer. N Engl J Med 2004;351:337–45.
8. Saltz LB, Meropol NJ, Loehrer PJ, et al. Phase II trial of cetuximab in patients with refractory colorectal cancer that expresses the epidermal growth factor receptor. J Clin Oncol 2004;22:1201–8.
9. Grandis JR, Drenning SD, Chakraborty A, et al. Requirement of Stat3 but not Stat1 activation for epidermal growth factor receptor- mediated cell growth *in vitro*. J Clin Invest 1998;102:1385–92.
10. Olayioye MA, Beuvink I, Horsch K, Daly JM, Hynes NE. ErbB receptor-induced activation of stat transcription factors is mediated by Src tyrosine kinases. J Biol Chem 1999;274:17209–18.
11. Biscardi JS, Maa MC, Tice DA, et al. c-Src-mediated phosphorylation of the epidermal growth factor receptor on Tyr845 and Tyr1101 is associated with modulation of receptor function. J Biol Chem 1999; 274:8335–43.
12. Barré B, Vigneron A, Coqueret O. The STAT3 transcription factor is a target for the Myc and retinoblastoma proteins on the Cdc25A promoter. J Biol Chem 2005;280:15673–81.
13. Leslie K, Lang C, Devgan G, et al. Cyclin D1 is transcriptionally regulated by and required for transformation by activated signal transducer and activator of transcription 3. Cancer Res 2006;66:2544–52.
14. Kiuchi N, Nakajima K, Ichiba M, et al. STAT3 is required for the gp130-mediated full activation of the c-myc gene. J Exp Med 1999;189:63–73.
15. Shirogane T, Fukada T, Muller JM, et al. Synergistic roles for Pim-1 and c-Myc in STAT3-mediated cell cycle progression and antiapoptosis. Immunity 1999;11: 709–19.
16. Bromberg J, Wrzeszczynska M, Devgan G, et al. Stat3 as an oncogene. Cell 1999;98:295–303.
17. Ivanov VN, Bhoumik A, Krasilnikov M, et al. Cooperation between STAT3 and c-jun suppresses Fas transcription. Mol Cell 2001;7:517–28.
18. Catlett-Falcone R, Landowski TH, Oshiro M, et al.

Constitutive activation of Stat3 signaling confers resistance to apoptosis in human U266 myeloma cells. Immunity 1999;10:105–15.
19. Dechow TN, Pedranzini L, Leitch A, et al. Requirement of matrix metalloproteinase-9 for the transformation of human mammary epithelial cells by Stat3-C. Proc Natl Acad Sci U S A 2004;101:10602–7.
20. Vigneron A, Roninson IB, Gamelin E, Coqueret O. Src inhibits adriamycin-induced senescence and G_2 checkpoint arrest by blocking the induction of p21waf1. Cancer Res 2005;65:8927–35.
21. Barre B, Vigneron A, Perkins N, et al. The STAT3 oncogene as a predictive marker of drug resistance. Trends Mol Med 2007;13:4–11.
22. Osman F, Whitby MC. Exploring the roles of Mus81-1/Mms4 at perturbed replication forks. DNA Repair (Amst) 2007;6:1004–17.
23. Bhonde MR, Hanski ML, Notter M, et al. Equivalent effect of DNA damage-induced apoptotic cell death or long-term cell cycle arrest on colon carcinoma cell proliferation and tumour growth. Oncogene 2006;25:165–75.
24. Gorgoulis VG, Pratsinis H, Zacharatos P, et al. p53-dependent ICAM-1 overexpression in senescent human cells identified in atherosclerotic lesions. Lab Invest 2005;85:502–11.
25. Gorgoulis VG, Zacharatos P, Kotsinas A, et al. p53 activates ICAM-1 (CD54) expression in an NF-κB-independent manner. EMBO J 2003;22:1567–78.
26. Pommier Y, Redon C, Rao VA, et al. Repair of and checkpoint response to topoisomerase I-mediated DNA damage. Mutat Res 2003;532:173–203.
27. Whitby MC. Junctions on the road to cancer. Nat Struct Mol Biol 2004;11:693–5.
28. Dendouga N, Gao H, Moechars D, et al. Disruption of murine Mus81 increases genomic instability and DNA damage sensitivity but does not promote tumorigenesis. Mol Cell Biol 2005;25:7569–79.
29. Johnstone RW, Ruefli AA, Lowe SW. Apoptosis: a link between cancer genetics and chemotherapy. Cell 2002;108:153–64.
30. Lee S, Schmitt CA. Chemotherapy response and resistance. Curr Opin Genet Dev 2003;13:90–6.
31. Masters JR, Koberle B. Curing metastatic cancer: lessons from testicular germ-cell tumours. Nat Rev Cancer 2003;3:517–25.
32. Hiyama T, Katsura M, Yoshihara T, et al. Haploinsufficiency of the Mus81-1 endonuclease activates the intra-S-phase and G_2-M checkpoints and promotes rereplication in human cells. Nucleic Acids Res 2006;34:880–92.
33. Tao W, South VJ, Zhang Y, et al. Induction of apoptosis by an inhibitor of the mitotic kinesin KSP requires both activation of the spindle assembly checkpoint and mitotic slippage. Cancer Cell 2005;8:49–59.
34. Andreassen PR, Lacroix FB, Lohez OD, Margolis RL. Neither p21WAF1 nor 14-3-3σ prevents G_2 progression to mitotic catastrophe in human colon carcinoma cells after DNA damage, but p21WAF1 induces stable G_1 arrest in resulting tetraploid cells. Cancer Res 2001;61:7660–8.
35. Weaver BA, Cleveland DW. Decoding the links between mitosis, cancer, and chemotherapy: the mitotic checkpoint, adaptation, and cell death. Cancer Cell 2005;8:7–12.
36. Fischer OM, Hart S, Gschwind A, Prenzel N, Ullrich A. Oxidative and osmotic stress signaling in tumor cells is mediated by ADAM proteases and heparin-binding epidermal growth factor. Mol Cell Biol 2004;24:5172–83.
37. Winograd-Katz SE, Levitzki A. Cisplatin induces PKB/Akt activation and p38(MAPK) phosphorylation of the EGF receptor. Oncogene 2006;25:7381–90.

The EGFR-STAT3 Oncogenic Pathway Up-regulates the Eme1 Endonuclease to Reduce DNA Damage after Topoisomerase I Inhibition

Arnaud Vigneron, Erick Gamelin and Olivier Coqueret

Cancer Res 2008;68:815-825.